Supplementary material for

Statistical precursor signals for Dansgaard-Oeschger cooling transitions

Takahito Mitsui* and Niklas Boers

December 18, 2023

*Corresponding author. Email: takahito321@gmail.com

This PDF file includes:

Table S1 Durations of 12 Greenland interstadials longer than 1000 years analyzed in this study (Rasmussen et al., 2014).

Interstadial	Duration (yr)	Duration after excluding 2σ uncertainty range of the event timing
GI-25	4730	4570
GI-24.2	1380	1220
GI-24.1	1310	1150
GI-23.1-22	16440	16280
GI-21.1	7000	6760
GI-20	2340	2180
GI-19.2	1960	1520
GI-16.1	1540	1380
GI-14-13	5880	5640
GI-12	2580	2420
GI-8	1640	1480
GI-1	1796	1796

Table S2 The number of positive trends and significantly positive trends in the variance and lag-1 autocorrelation time series of Greenland ice cores.

Greenland ice cores	CSD indicator	Total cases	Positive trends	Significantly positive
NGRIP δ^{18}O	variance	12	9	6
NGRIP δ^{18}O	lag-1 autocorrelation	12	10	2
GRIP δ^{18}O	variance	9	8	4
GRIP δ^{18}O	lag-1 autocorrelation	9	6	2
GISP2 δ^{18}O	variance	9	6	6
GISP2 δ^{18}O	lag-1 autocorrelation	9	5	0
NGRIP $\log_{10}[Ca^{2+}]$	variance	10	5	4
NGRIP $\log_{10}[Ca^{2+}]$	lag-1 autocorrelation	10	9	2
GRIP $\log_{10}[Ca^{2+}]$	variance	9	8	3
GRIP $\log_{10}[Ca^{2+}]$	lag-1 autocorrelation	9	9	4
GISP2 $\log_{10}[Ca^{2+}]$	variance	9	6	2
GISP2 $\log_{10}[Ca^{2+}]$	lag-1 autocorrelation	9	8	2

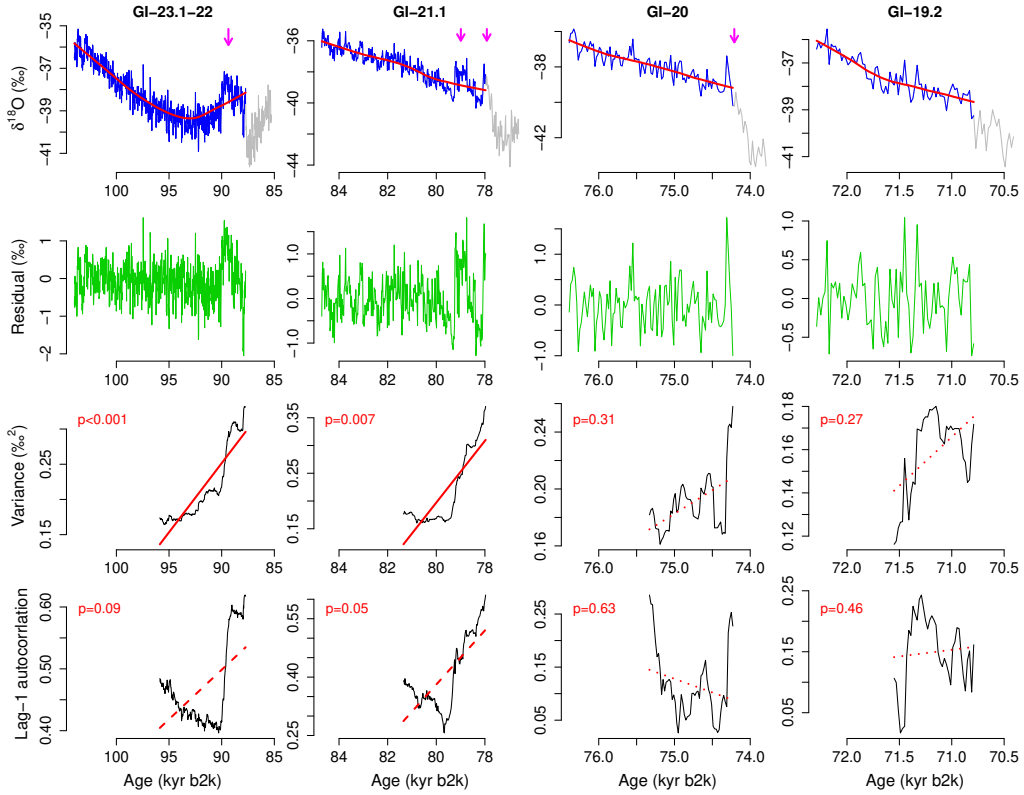

Figure S1. Analysis of CSD-based precursor signals of abrupt DO cooling transitions, for the first 4 interstadials of GRIP δ^{18}O, from 115 ka to 70.5 kyr b2k. (Top row) Interstadials longer than 1000 yr (blue). The cooling transition and stadial parts are shown in grey (Rasmussen et al., 2014). Nonlinear trends are calculated with the Locally Weighted Scatterplot Smoothing (LOESS) (red). The smoothing span α that defines the fraction of data points involved in the local regression is set to 50% of each interstadial length. The rebound events are indicated by arrows (see Section 2.1). (Second row) Residuals (green) resulting from subtracting the nonlinear trends (red) from the records (blue). (Third row) Variance estimate in rolling windows (black) with size equal to 50% of each interstadial length. Values are plotted at the right edge of each rolling window. The linear trend is shown by a solid red line for $p < 0.05$, by a dashed red line for $0.05 < p < 0.1$, and by a dotted line for $p > 0.1$. (Fourth row) Same as third row but for the lag-one autocorrelation (i.e., a lag of 20 yr).

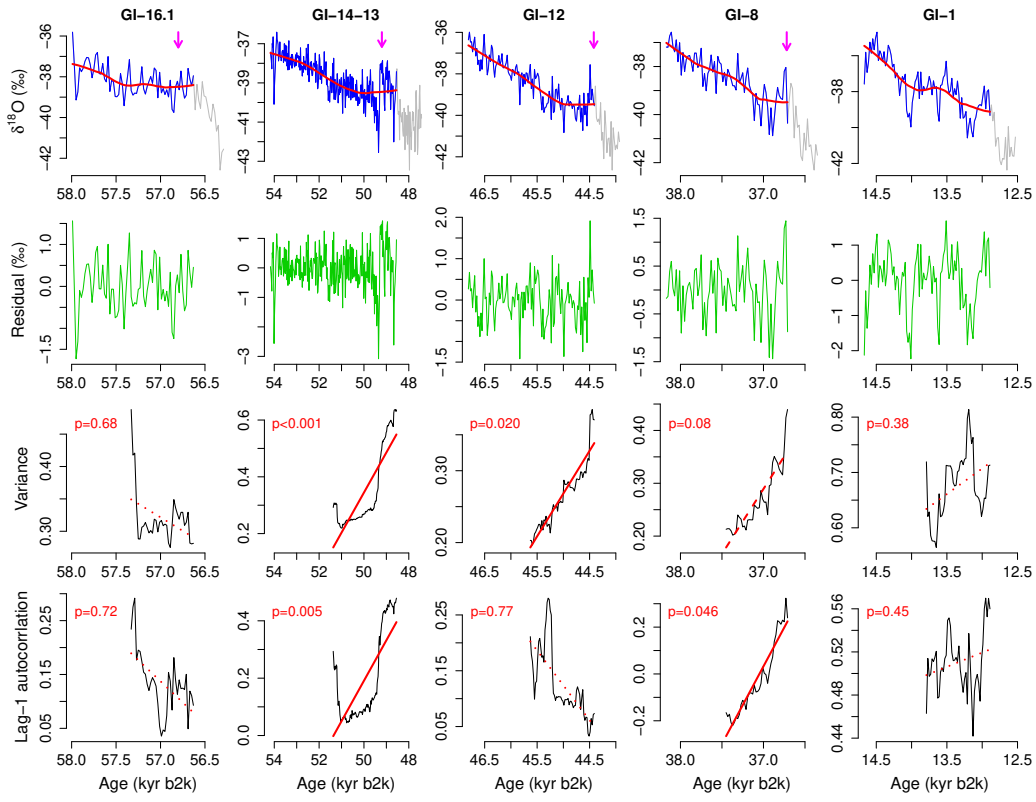

Figure S2. Same as Fig. S1 but for the following 5 interstadials, from 58 ka to 12 kyr b2k.

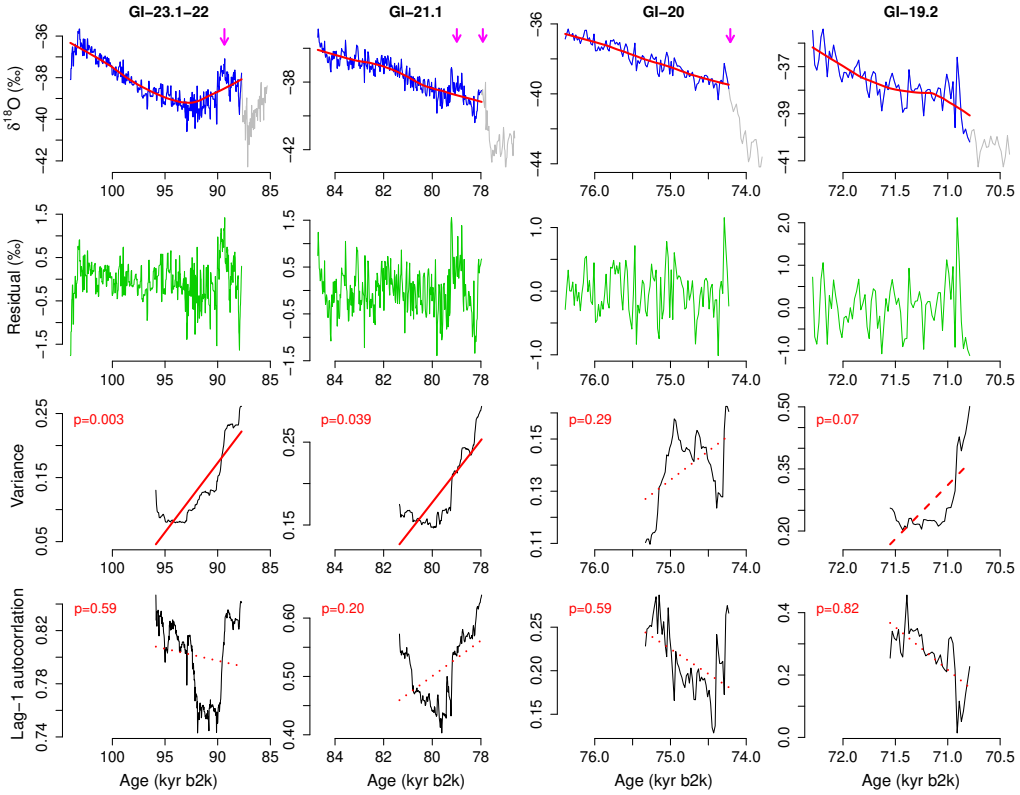

Figure S3. Analysis of CSD-based precursor signals of abrupt DO cooling transitions, for the first 4 interstadials of GISP2 δ^{18}O, from 115 ka to 70.5 kyr b2k. (Top row) Interstadials longer than 1000 yr (blue). The cooling transition and stadial parts are shown in grey (Rasmussen et al., 2014). Nonlinear trends are calculated with the Locally Weighted Scatterplot Smoothing (LOESS) (red). The smoothing span α that defines the fraction of data points involved in the local regression is set to 50% of each interstadial length. The rebound events are indicated by arrows (see Section 2.1). (Second row) Residuals (green) resulting from subtracting the nonlinear trends (red) from the records (blue). (Third row) Variance estimate in rolling windows (black) with size equal to 50% of each interstadial length. Values are plotted at the right edge of each rolling window. The linear trend is shown by a solid red line for $p < 0.05$, by a dashed red line for $0.05 < p < 0.1$, and by a dotted line for $p > 0.1$. (Fourth row) Same as third row but for the lag-one autocorrelation (i.e., a lag of 20 yr).

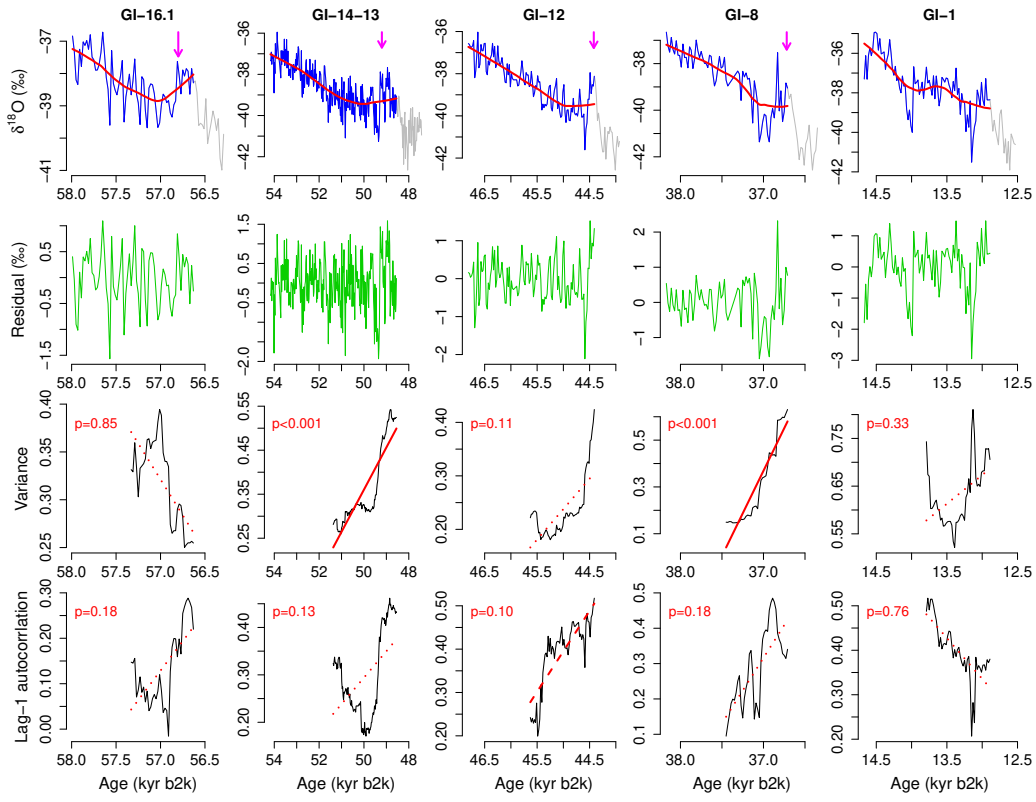

Figure S4. Same as Fig. S3 but for the following 5 interstadials, from 58 ka to 12 kyr b2k.

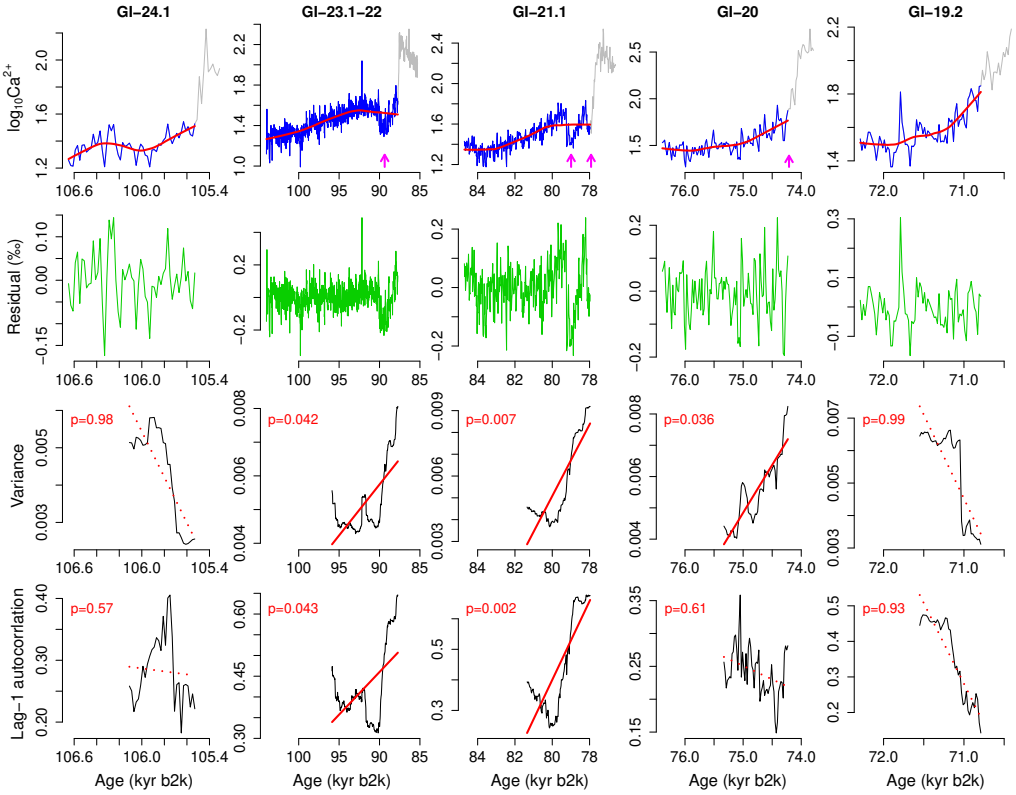

Figure S5. Analysis of CSD-based precursor signals of abrupt DO cooling transitions, for the first 5 interstadials of NGRIP $\log_{10}[Ca^{2+}]$, from 115 ka to 70.5 kyr b2k. (Top row) Interstadials longer than 1000 yr (blue). The cooling transition and stadial parts are shown in grey (Rasmussen et al., 2014). Nonlinear trends are calculated with the Locally Weighted Scatterplot Smoothing (LOESS) (red). The smoothing span α that defines the fraction of data points involved in the local regression is set to 50% of each interstadial length. The rebound events are indicated by arrows (see Section 2.1). (Second row) Residuals (green) resulting from subtracting the nonlinear trends (red) from the records (blue). (Third row) Variance estimate in rolling windows (black) with size equal to 50% of each interstadial length. Values are plotted at the right edge of each rolling window. The linear trend is shown by a solid red line for $p < 0.05$, by a dashed red line for $0.05 < p < 0.1$, and by a dotted line for $p > 0.1$. (Fourth row) Same as third row but for the lag-one autocorrelation (i.e., a lag of 20 yr).

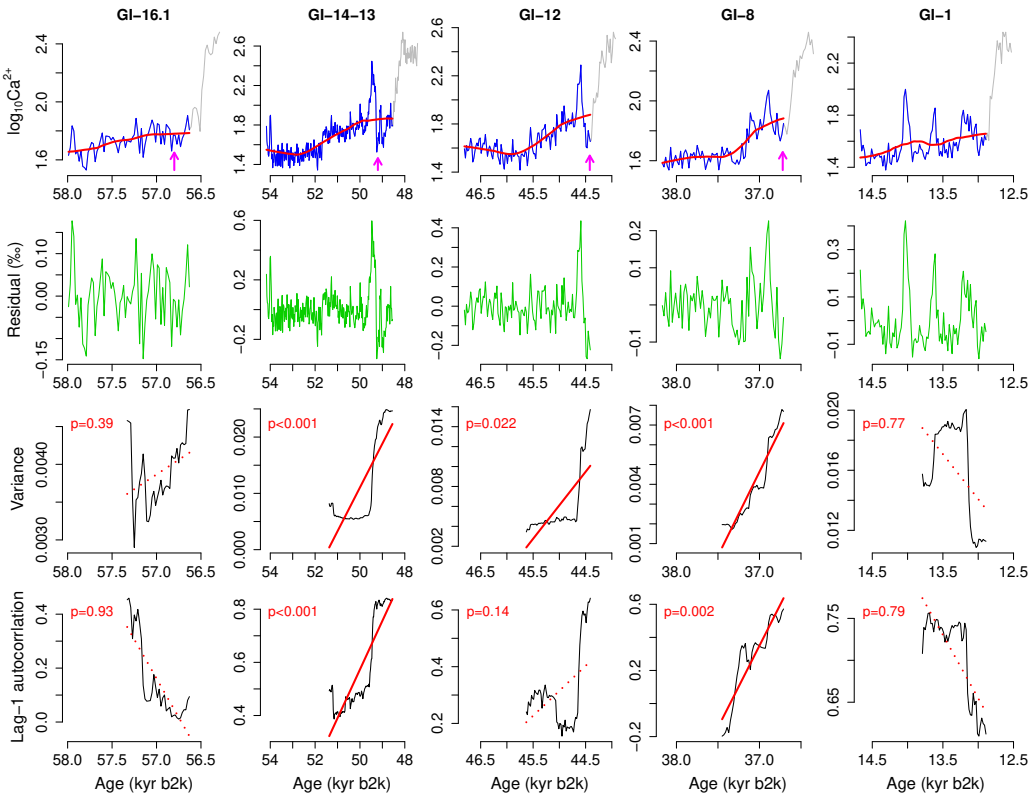

Figure S6. Same as Fig. S5 but for the following 5 interstadials, from 58 ka to 12 kyr b2k.

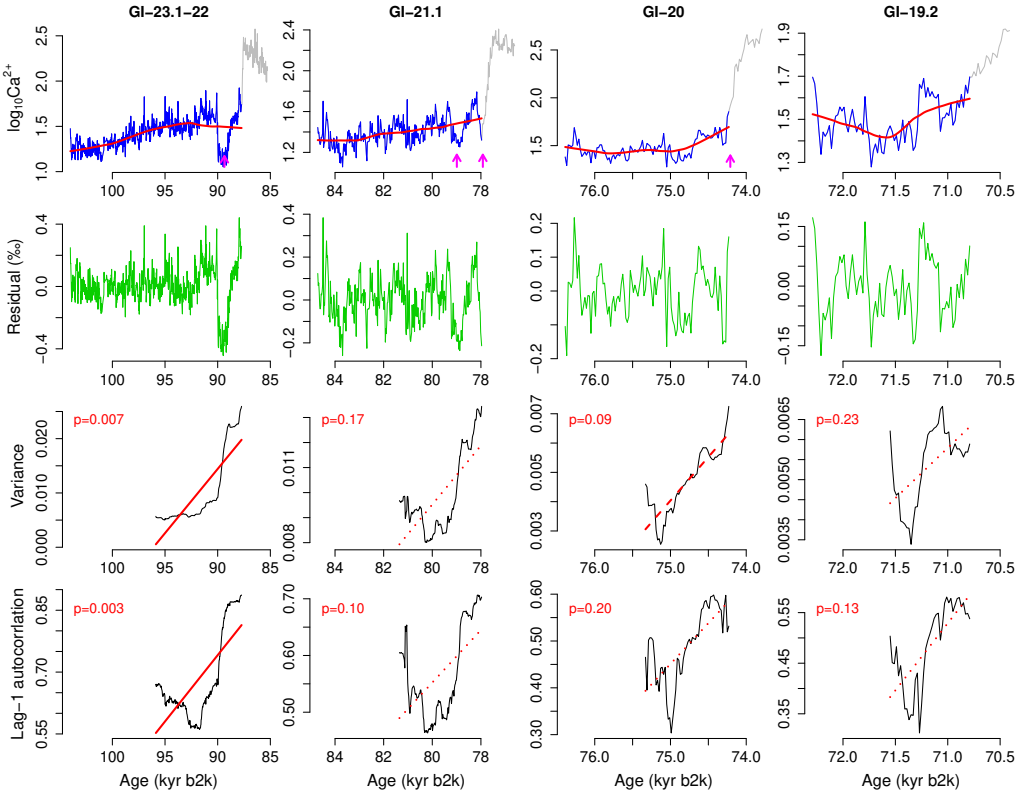

Figure S7. Analysis of CSD-based precursor signals of abrupt DO cooling transitions, for the first 4 interstadials of GRIP $\log_{10}[Ca^{2+}]$, from 115 ka to 70.5 kyr b2k. (Top row) Interstadials longer than 1000 yr (blue). The cooling transition and stadial parts are shown in grey (Rasmussen et al., 2014). Nonlinear trends are calculated with the Locally Weighted Scatterplot Smoothing (LOESS) (red). The smoothing span α that defines the fraction of data points involved in the local regression is set to 50% of each interstadial length. The rebound events are indicated by arrows (see Section 2.1). (Second row) Residuals (green) resulting from subtracting the nonlinear trends (red) from the records (blue). (Third row) Variance estimate in rolling windows (black) with size equal to 50% of each interstadial length. Values are plotted at the right edge of each rolling window. The linear trend is shown by a solid red line for $p < 0.05$, by a dashed red line for $0.05 < p < 0.1$, and by a dotted line for $p > 0.1$. (Fourth row) Same as third row but for the lag-one autocorrelation (i.e., a lag of 20 yr).

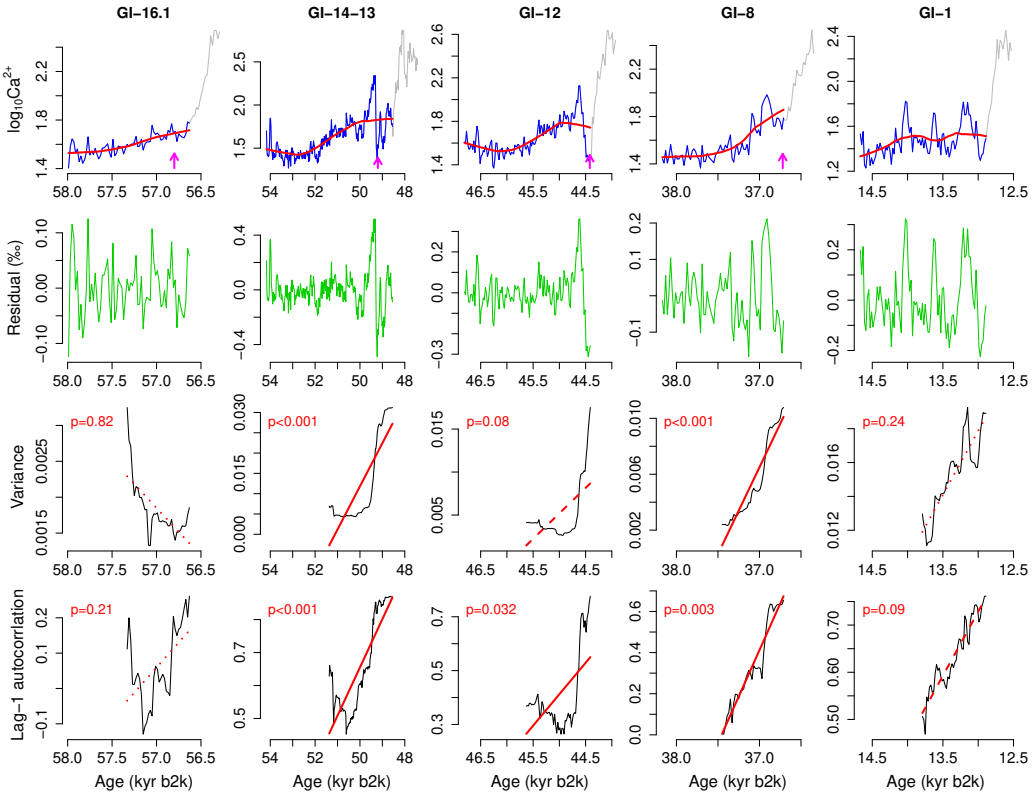

Figure S8. Same as Fig. S7 but for the following 5 interstadials, from 58 ka to 12 kyr b2k.

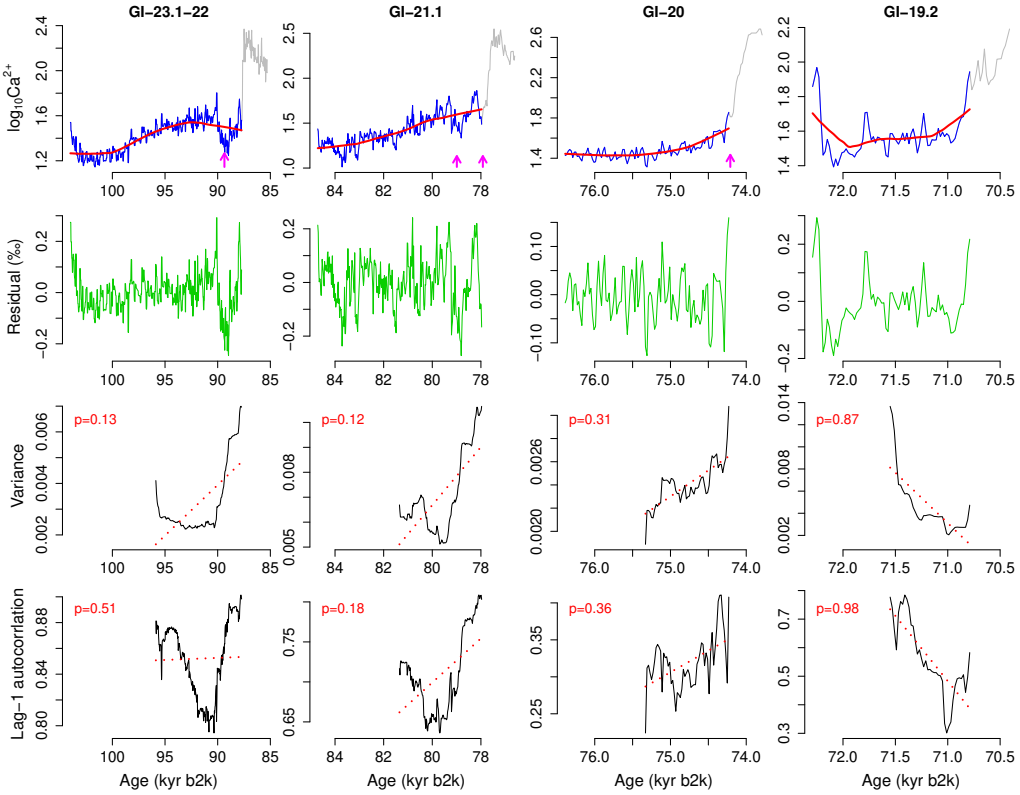

Figure S9. Analysis of CSD-based precursor signals of abrupt DO cooling transitions, for the first 4 interstadials of GISP2 $\log_{10}[Ca^{2+}]$, from 115 ka to 70.5 kyr b2k. (Top row) Interstadials longer than 1000 yr (blue). The cooling transition and stadial parts are shown in grey (Rasmussen et al., 2014). Nonlinear trends are calculated with the Locally Weighted Scatterplot Smoothing (LOESS) (red). The smoothing span α that defines the fraction of data points involved in the local regression is set to 50% of each interstadial length. The rebound events are indicated by arrows (see Section 2.1). (Second row) Residuals (green) resulting from subtracting the nonlinear trends (red) from the records (blue). (Third row) Variance estimate in rolling windows (black) with size equal to 50% of each interstadial length. Values are plotted at the right edge of each rolling window. The linear trend is shown by a solid red line for $p < 0.05$, by a dashed red line for $0.05 < p < 0.1$, and by a dotted line for $p > 0.1$. (Fourth row) Same as third row but for the lag-one autocorrelation (i.e., a lag of 20 yr).

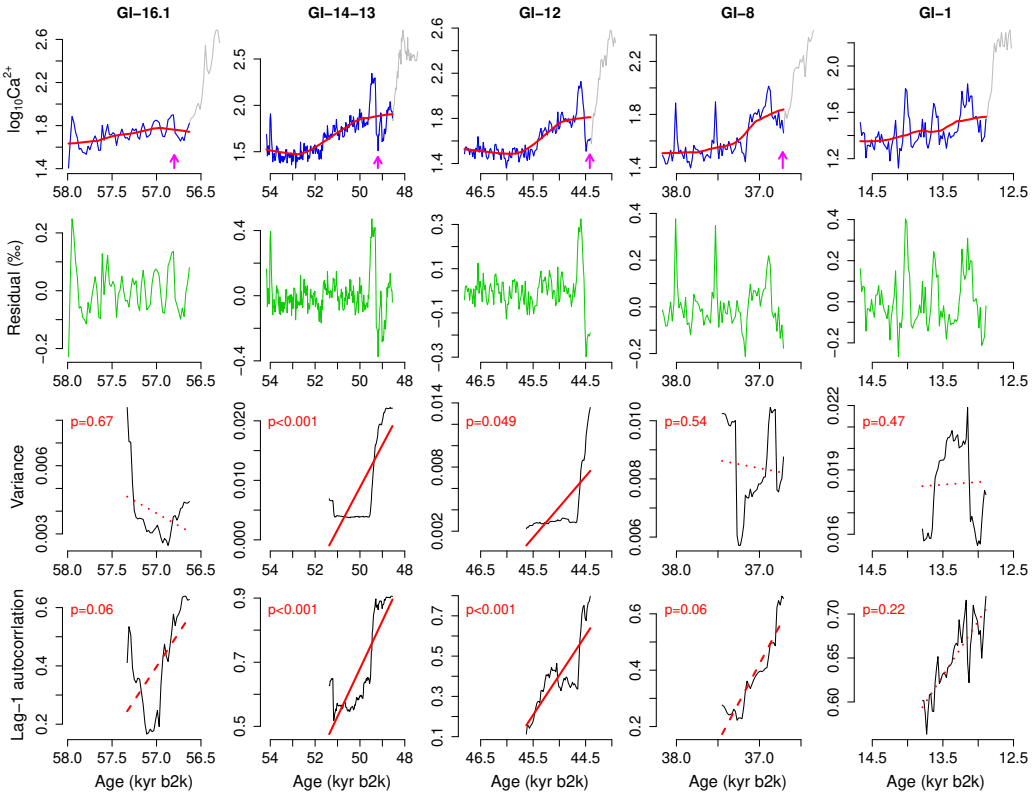

Figure S10. Same as Fig. S9 but for the following 5 interstadials, from 58 ka to 12 kyr b2k.

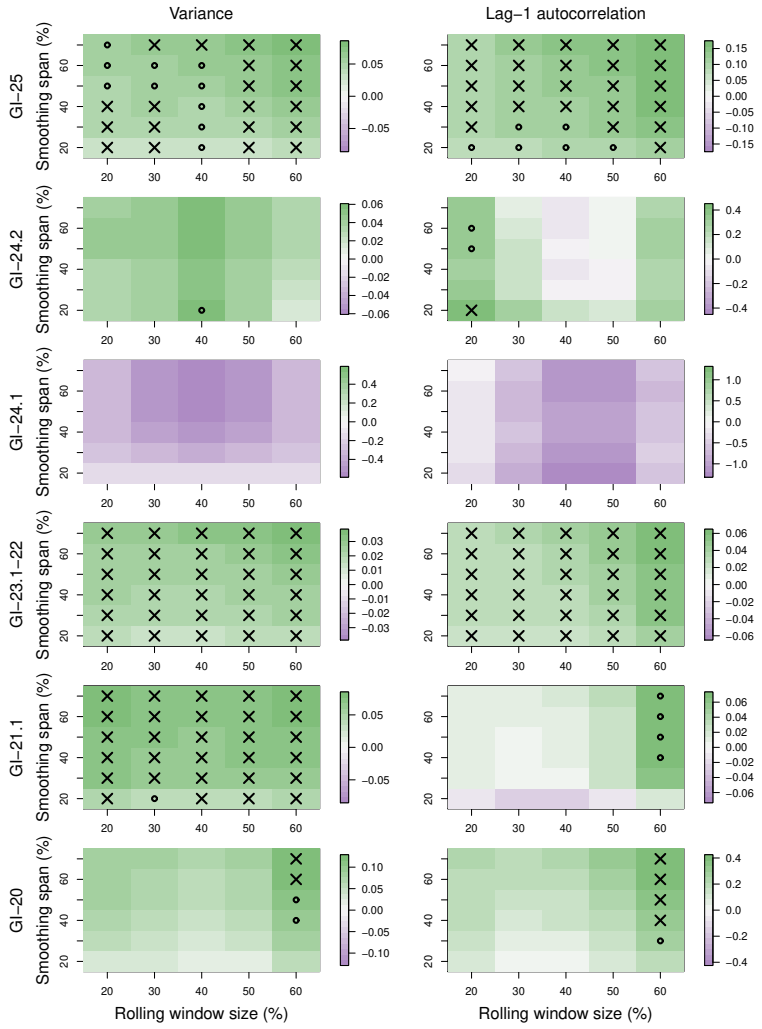

Figure S11. Robustness analysis for calculating the CSD indicators used to anticipate critical transitions, with respect to the smoothing span and the rolling window size (% of each interstadial length): the case of the first half of interstadials from NGRIP δ^{18}O record. Variance (left column) and lag-1 autocorrelation (right column). The color bar shows the trend value. The cross mark (x) indicates significantly positive trends ($p < 0.05$), the small open circle (o) indicates barely significant positive trends ($0.05 < p < 0.1$) and the cell is left blank if $p > 0.1$.

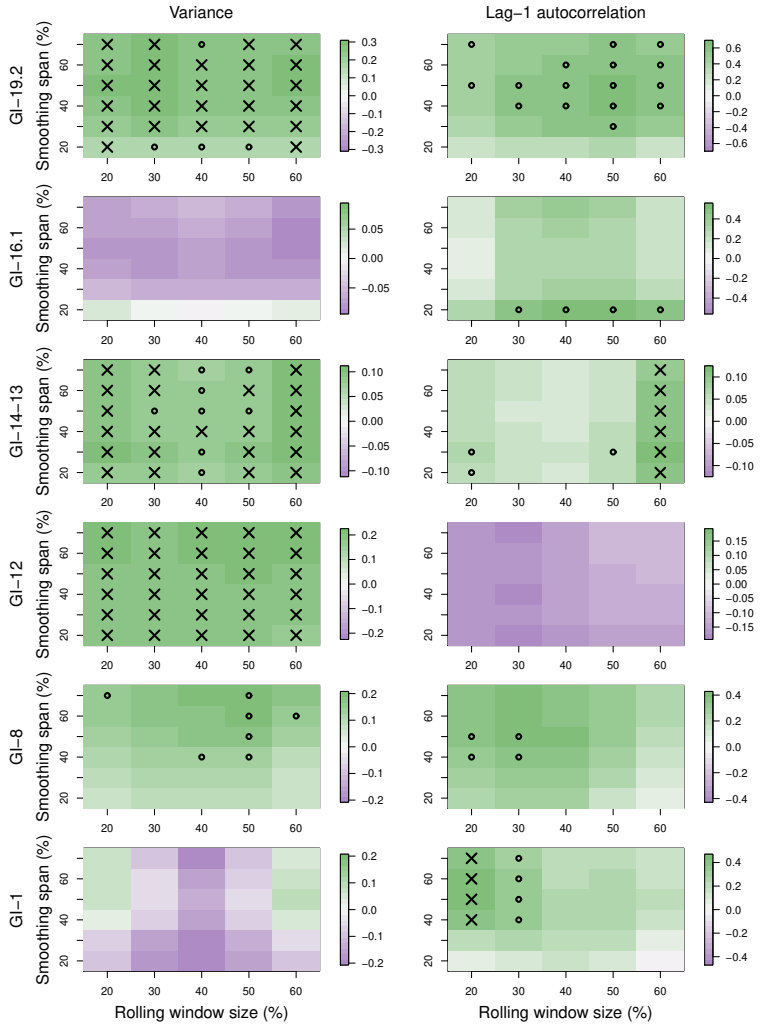

Figure S12. Same as Fig. S11 but for the second half of interstadials from NGRIP δ^{18}O record.

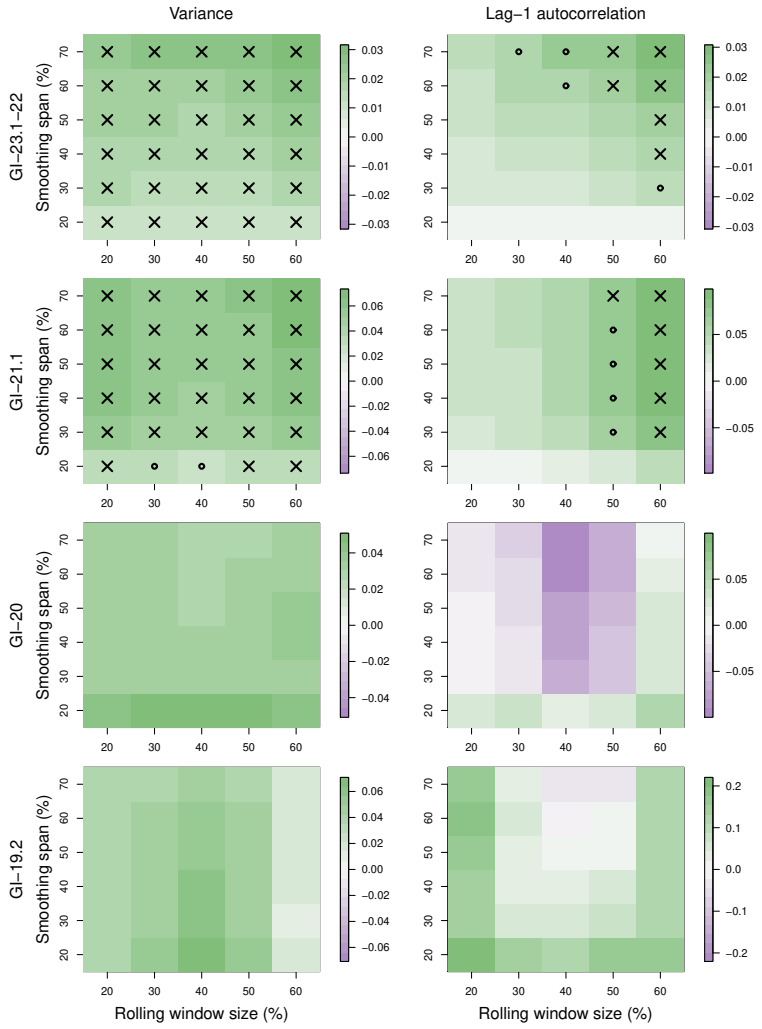

Figure S13. Robustness analysis for calculating the CSD indicators used to anticipate critical transitions, with respect to the smoothing span and the rolling window size (% of each interstadial length): the case of the first half of interstadials from GRIP δ^{18}O record. Variance (left column) and lag-1 autocorrelation (right column). The color bar shows the trend value. The cross mark (x) indicates significantly positive trends ($p < 0.05$), the small open circle (o) indicates barely significant positive trends ($0.05 < p < 0.1$) and the cell is left blank if $p > 0.1$.

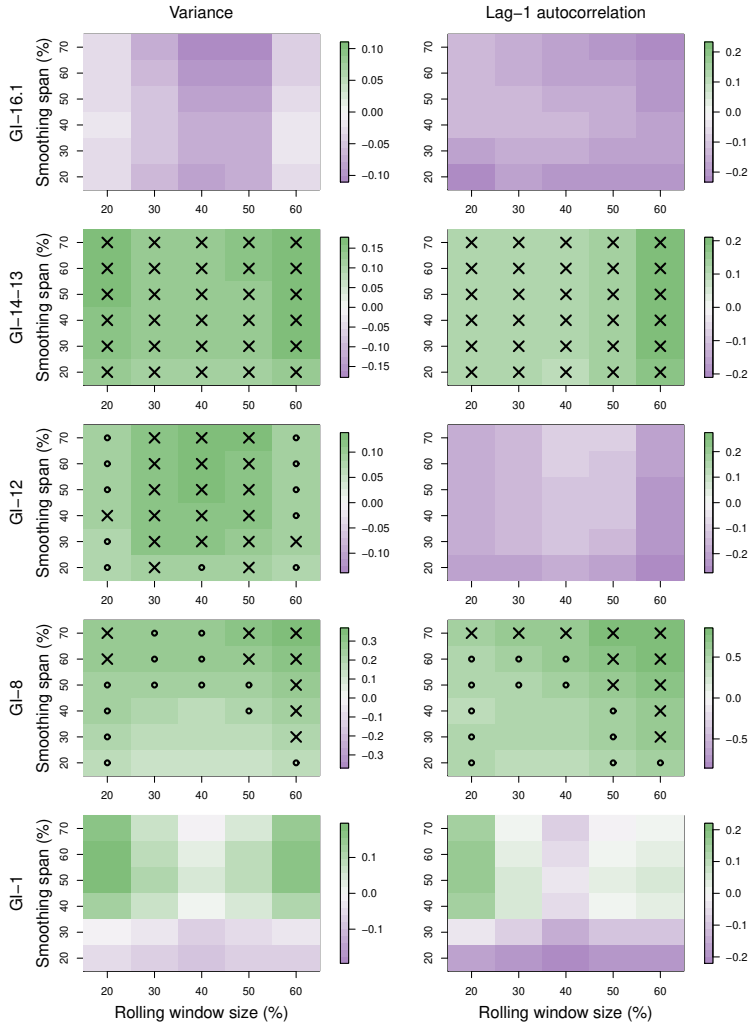

Figure S14. Same as Fig. S13 but for the second half of interstadials from GRIP δ^{18}O record.

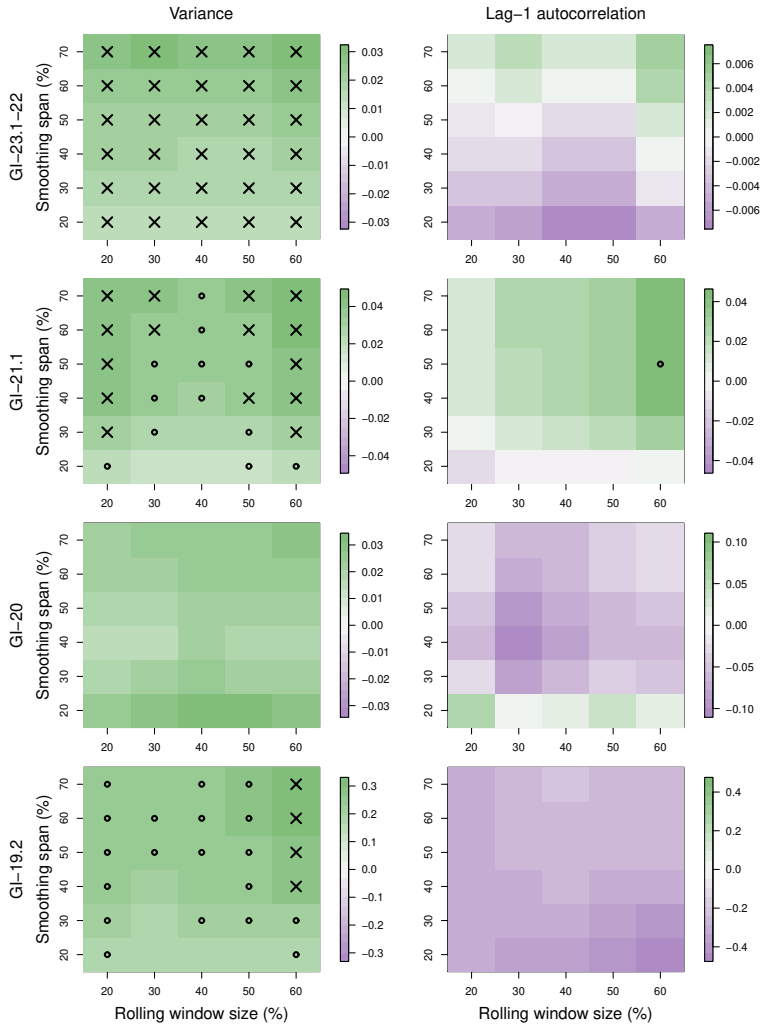

Figure S15. Robustness analysis for calculating the CSD indicators used to anticipate critical transitions, with respect to the smoothing span and the rolling window size (% of each interstadial length): the case of the first half of interstadials from GISP2 δ^{18}O record. Variance (left column) and lag-1 autocorrelation (right column). The color bar shows the trend value. The cross mark (x) indicates significantly positive trends ($p < 0.05$), the small open circle (o) indicates barely significant positive trends ($0.05 < p < 0.1$) and the cell is left blank if $p > 0.1$.

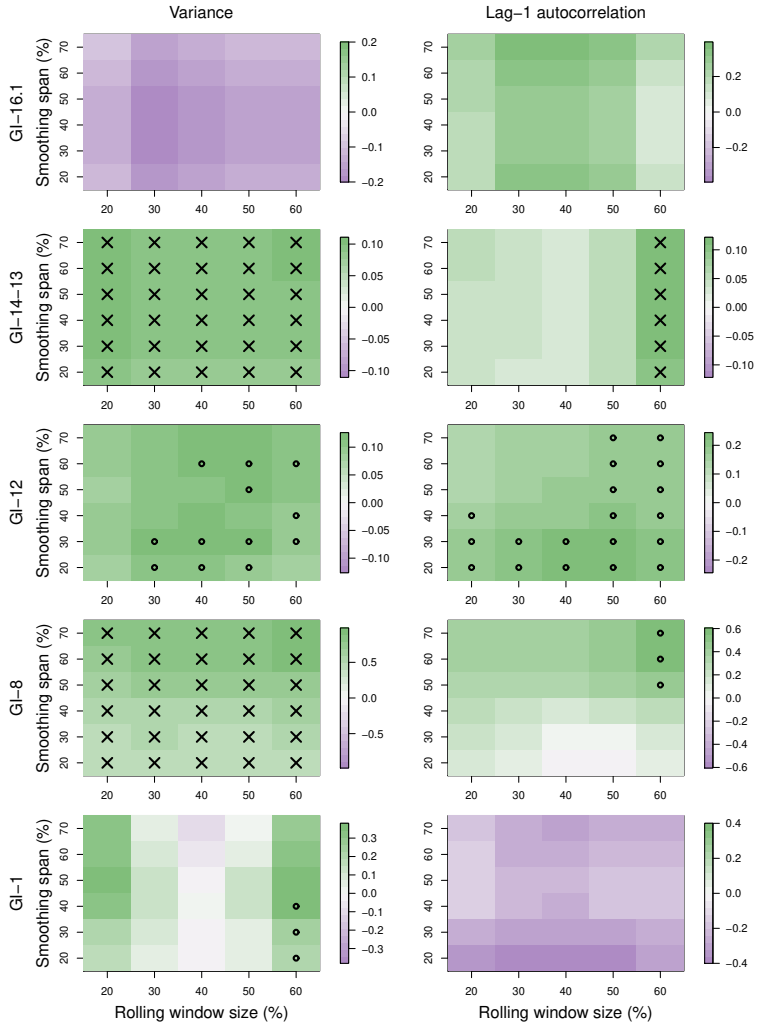

Figure S16. Same as Fig. S15 but for the second half of interstadials from GISP2 δ^{18}O record.

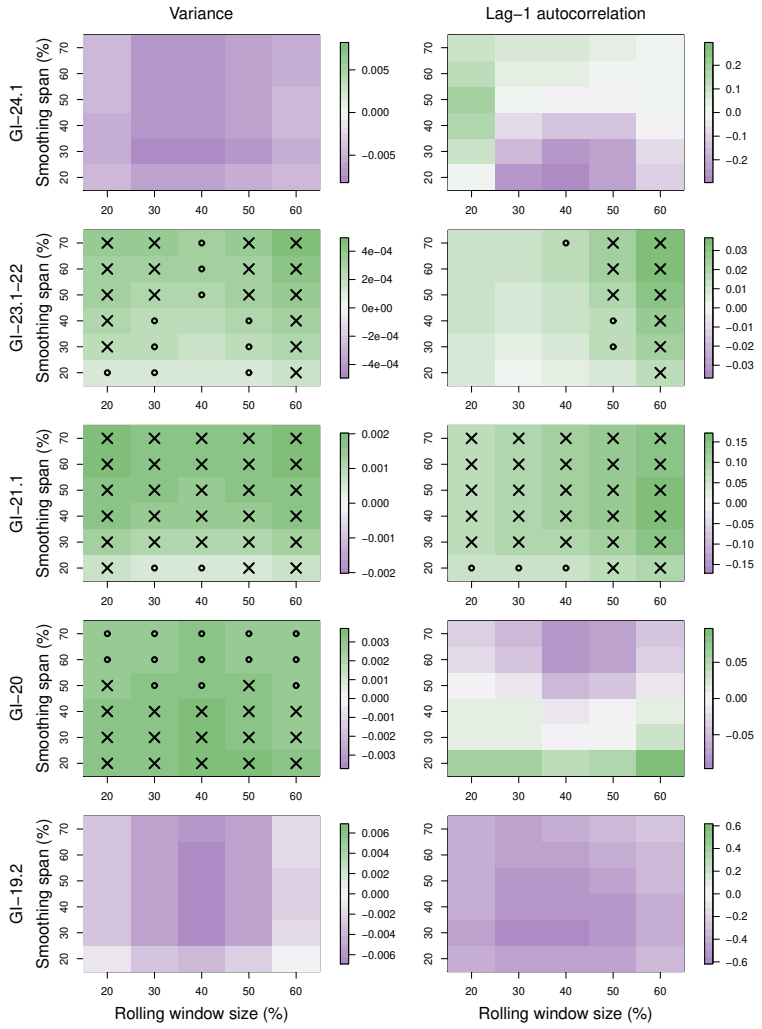

Figure S17. Robustness analysis for calculating the CSD indicators used to anticipate critical transitions, with respect to the smoothing span and the rolling window size (% of each interstadial length): the case of the first half of interstadials from NGRIP $\log_{10}[Ca^{2+}]$ record. Variance (left column) and lag-1 autocorrelation (right column). The color bar shows the trend value. The cross mark (x) indicates significantly positive trends ($p < 0.05$), the small open circle (o) indicates barely significant positive trends ($0.05 < p < 0.1$) and the cell is left blank if $p > 0.1$.

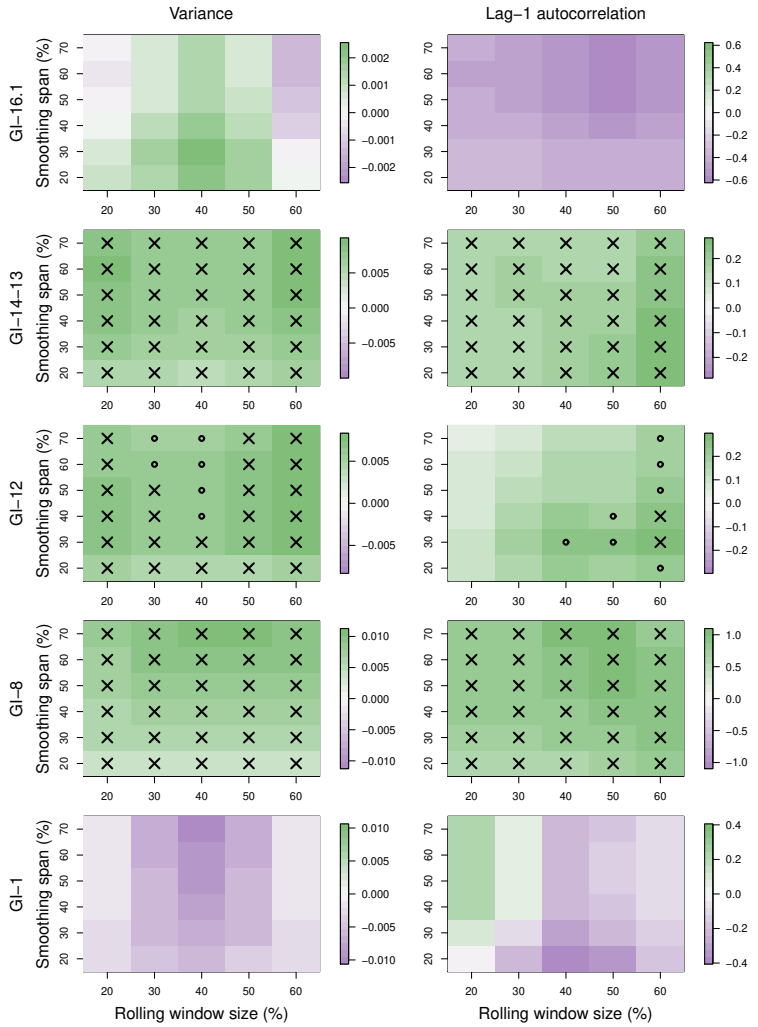

Figure S18. Same as Fig. S17 but for the second half of interstadials from NGRIP $\log_{10}[Ca^{2+}]$ record.

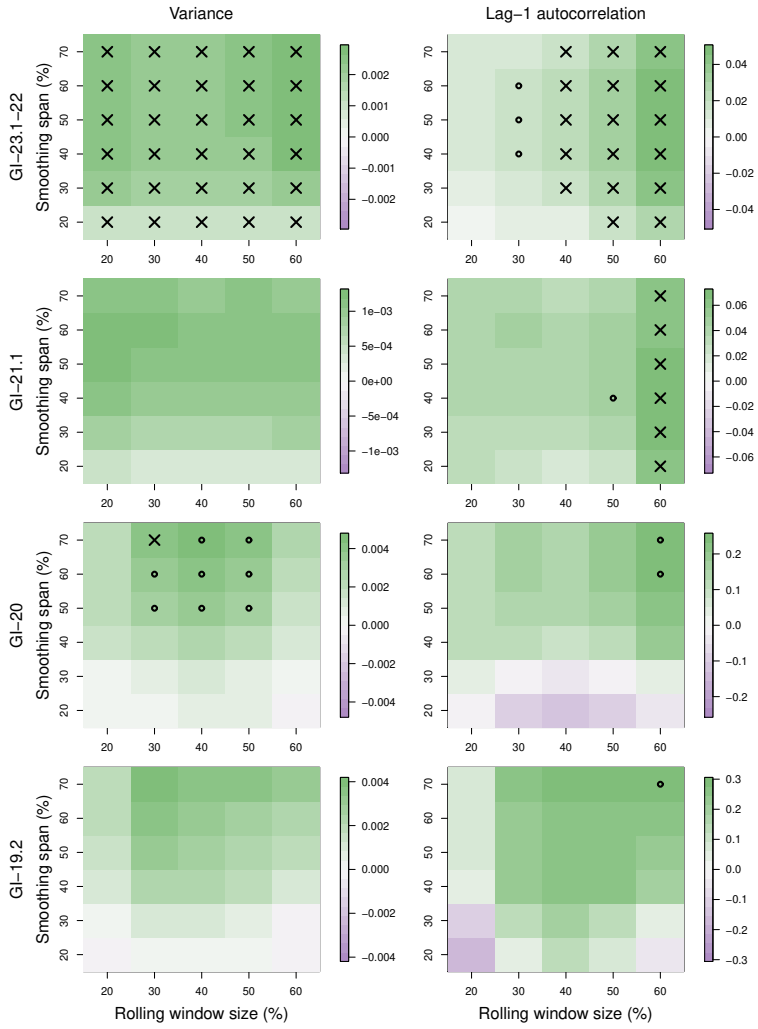

Figure S19. Robustness analysis for calculating the CSD indicators used to anticipate critical transitions, with respect to the smoothing span and the rolling window size (% of each interstadial length): the case of the first half of interstadials from GRIP $\log_{10}[Ca^{2+}]$ record. Variance (left column) and lag-1 autocorrelation (right column). The color bar shows the trend value. The cross mark (x) indicates significantly positive trends ($p < 0.05$), the small open circle (o) indicates barely significant positive trends ($0.05 < p < 0.1$) and the cell is left blank if $p > 0.1$.

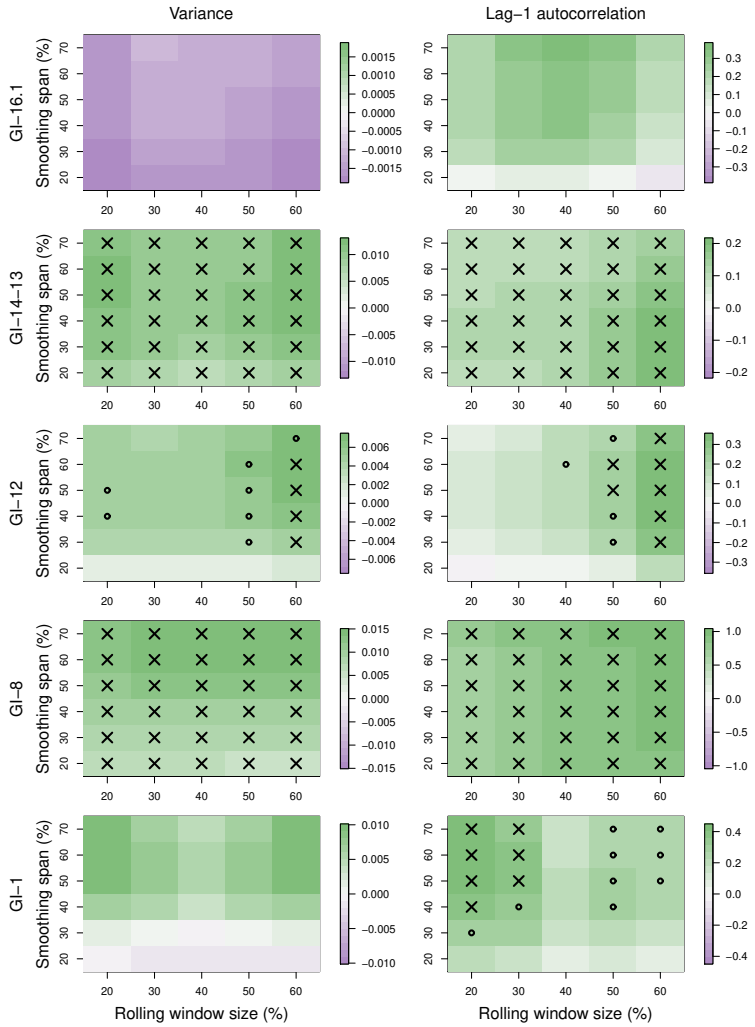

Figure S20. Same as Fig. S19 but for the second half of interstadials from GRIP $\log_{10}[Ca^{2+}]$ record.

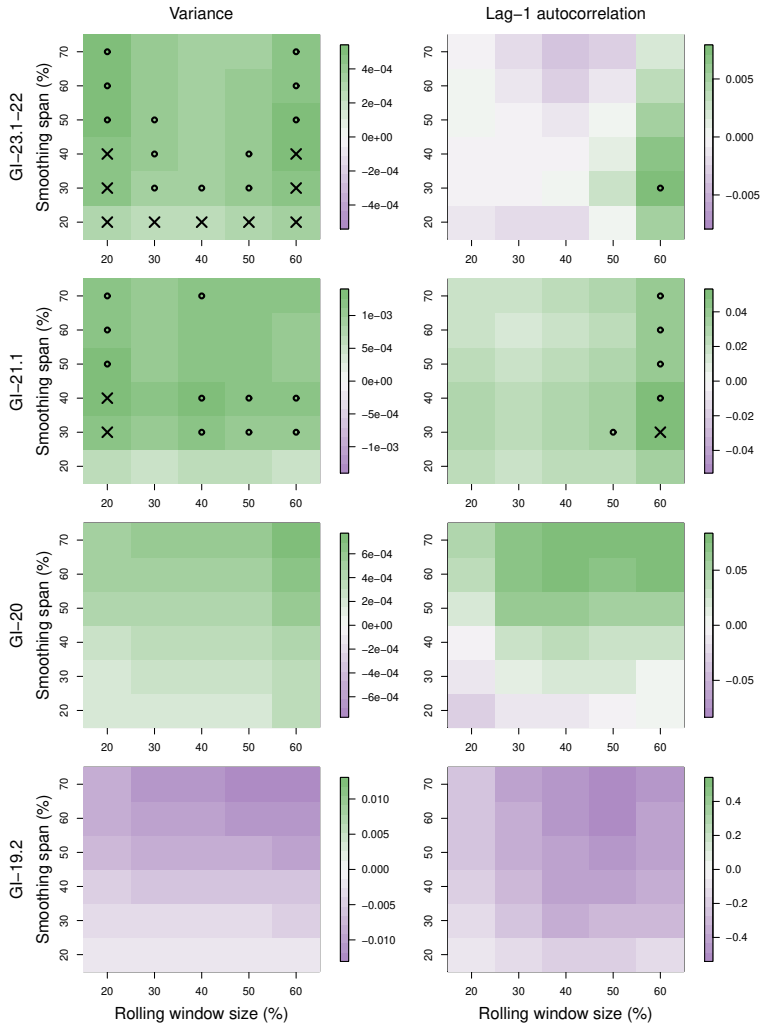

Figure S21. Robustness analysis for calculating the CSD indicators used to anticipate critical transitions, with respect to the smoothing span and the rolling window size (% of each interstadial length): the case of the first half of interstadials from GISP2 $\log_{10}[Ca^{2+}]$ record. Variance (left column) and lag-1 autocorrelation (right column). The color bar shows the trend value. The cross mark (x) indicates significantly positive trends ($p < 0.05$), the small open circle (o) indicates barely significant positive trends ($0.05 < p < 0.1$) and the cell is left blank if $p > 0.1$.

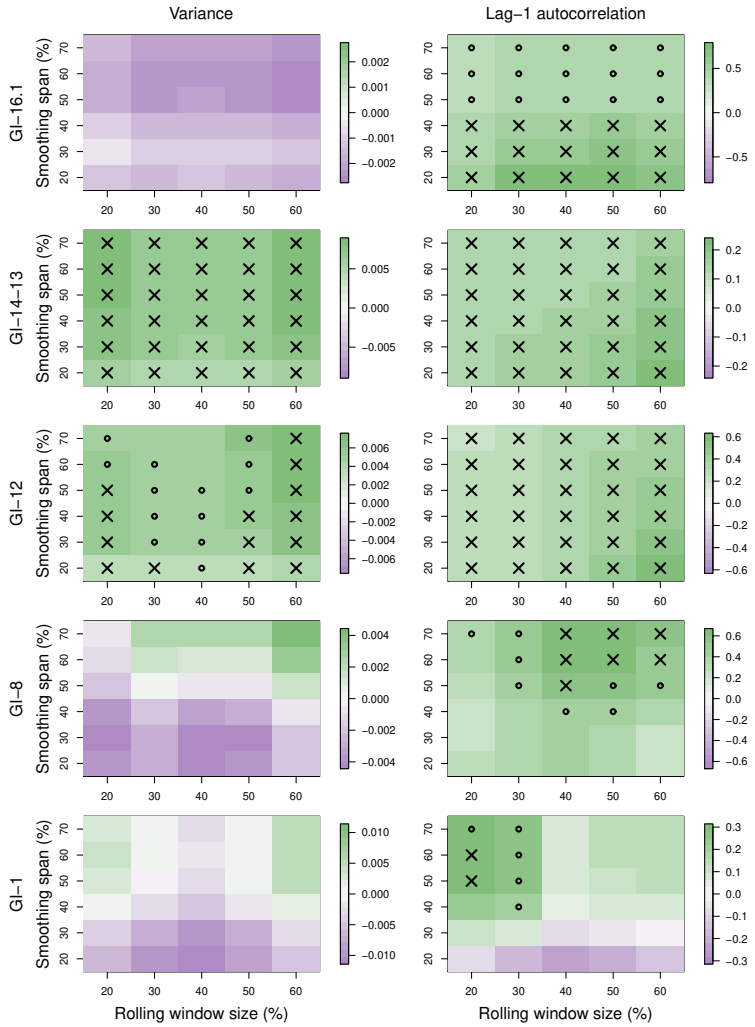

Figure S22. Same as Fig. S21 but for the second half of interstadials from GISP2 $\log_{10}[Ca^{2+}]$ record.

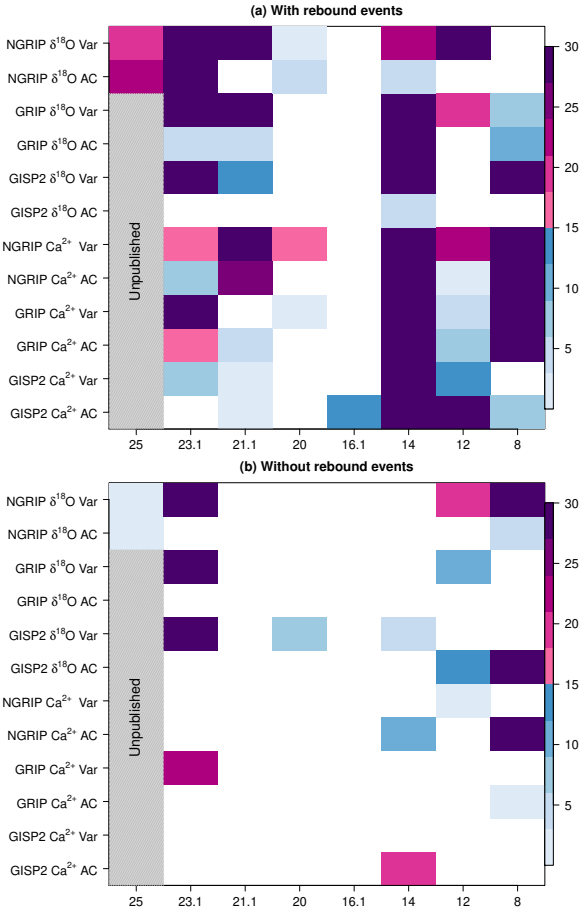

Figure S23. Detection of robust CSD-based precursor signals of DO cooling transitions with (a) and without (b) rebound events. Panel (a) is the same as Fig. 4(d) in the main text. The color indicates the number of detected significant trends of the CSD indicators ($p < 0.05$) for the 30 combinations of the smoothing span and the rolling window size. For the cases of grey-shaded cells, the data is not publicly available.

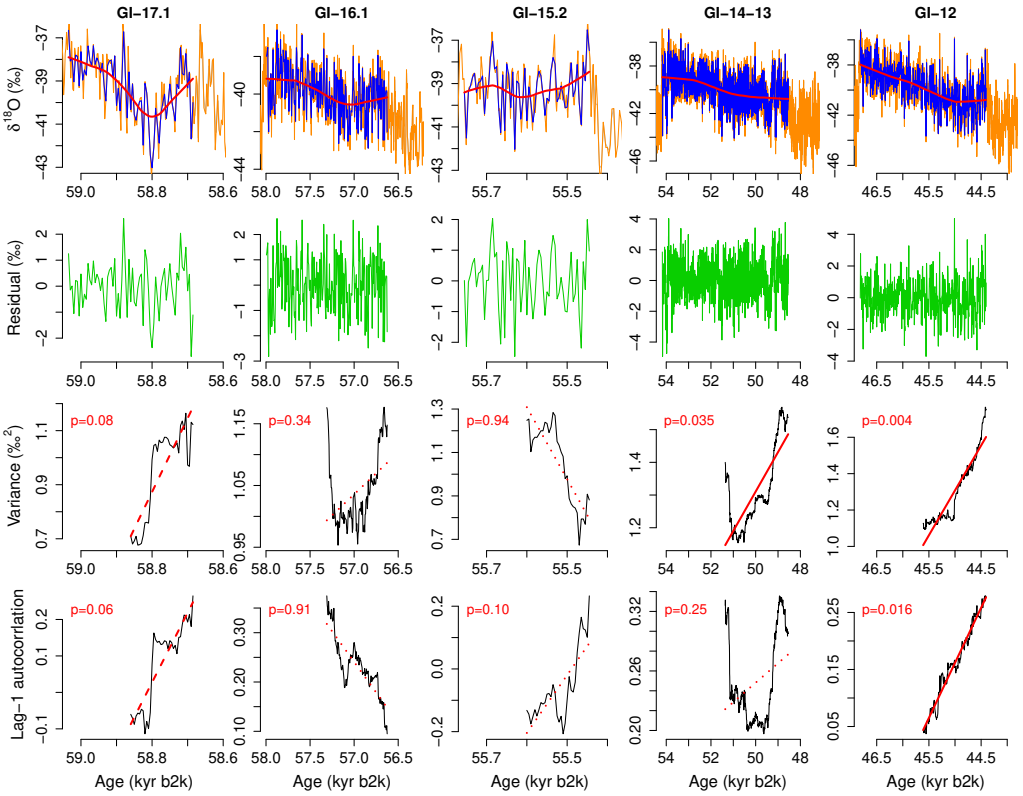

Figure S24. Analysis of CSD-based precursor signals of abrupt DO cooling transitions, for the first half of interglacials of 5-cm resolution NGRIP δ^{18}O. (Top row) Interstadial parts longer than 300-yr sampled at every 5-yr (blue) from the original data nonuniform in time (orange). The trend calculated with the Locally Weighted Scatterplot Smoothing (LOESS) (red). The smoothing span α that defines the fraction of data points involved in the local linear regression is set to $\alpha = 50\%$ of each interstadial length. (Second row) Residual (green) between the record and the trend. (Third row) Variance in the rolling window (black), size of which is 50% of each interstadial length. The linear trend is shown with the solid red line for $p < 0.05$, with the dashed line for $0.05 < p < 0.1$, and with the dotted line for $p > 0.1$. (Bottom row) Lag-1 autocorrelation.

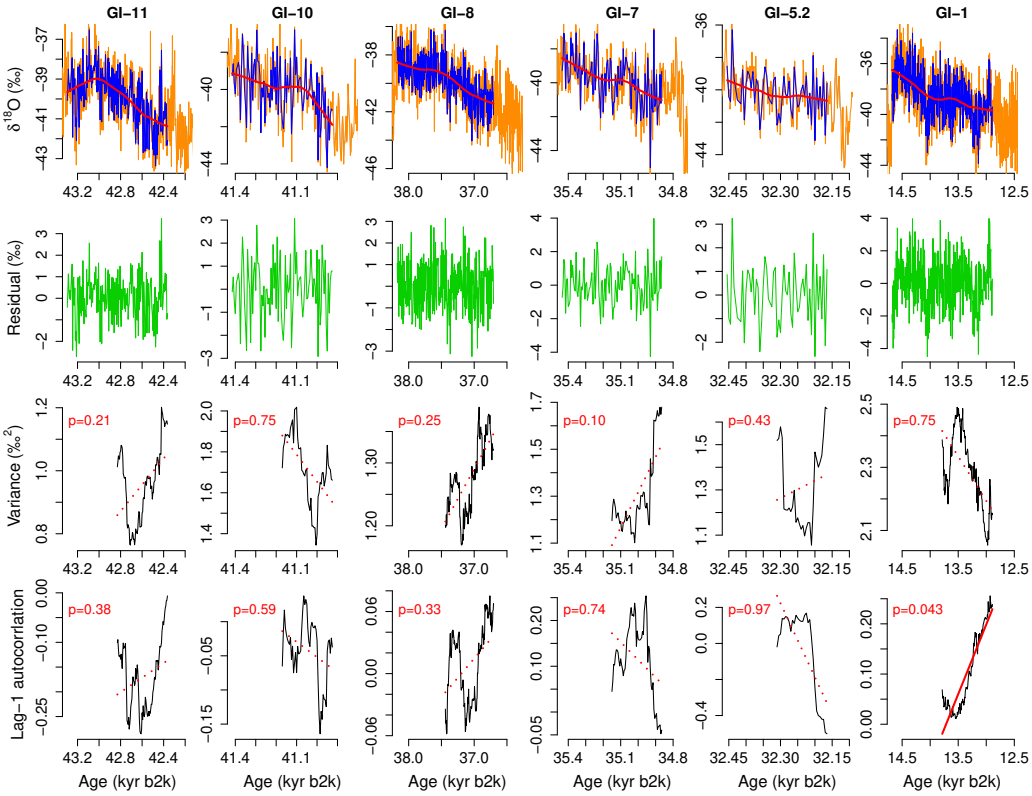

Figure S25. Analysis of CSD-based precursor signals of abrupt DO cooling transitions, for the second half of interglacials of 5-cm resolution NGRIP δ^{18}O. (Top row) Interstadial parts longer than 300-yr sampled at every 5-yr (blue) from the original data nonuniform in time (orange). The trend calculated with the Locally Weighted Scatterplot Smoothing (LOESS) (red). The smoothing span α that defines the fraction of data points involved in the local linear regression is set to $\alpha = 50\%$ of each interstadial length. (Second row) Residual (green) between the record and the trend. (Third row) Variance in the rolling window (black), size of which is 50% of each interstadial length. The linear trend is shown with the solid red line for $p < 0.05$, with the dashed line for $0.05 < p < 0.1$, and with the dotted line for $p > 0.1$. (Bottom row) Lag-1 autocorrelation.

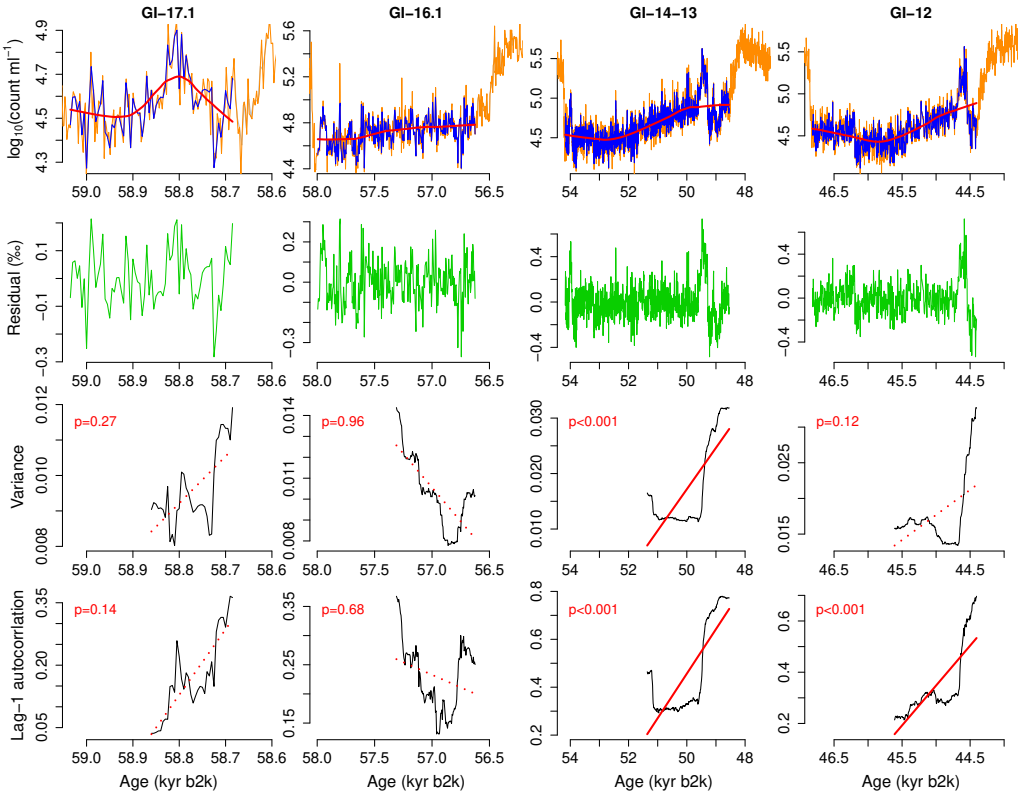

Figure S26. Analysis of CSD-based precursor signals of abrupt DO cooling transitions, for the first half of interglacials of NGRIP 5-cm resolution dust record. (Top row) Interstadial parts longer than 300-yr (blue), which is sampled at every 5-yr from the original data nonuniform in time (orange). The trend calculated with the Locally Weighted Scatterplot Smoothing (LOESS) (red). The smoothing span α that defines the fraction of data points involved in the local linear regression is set to $\alpha = 50\%$ of each interstadial length. (Second row) Residual (green) between the record and the trend. (Third row) Variance in the rolling window (black), size of which is 50% of each interstadial length. The linear trend is shown with the solid red line for $p < 0.05$, with the dashed line for $0.05 < p < 0.1$, and with the dotted line for $p > 0.1$. (Bottom row) Lag-1 autocorrelation.

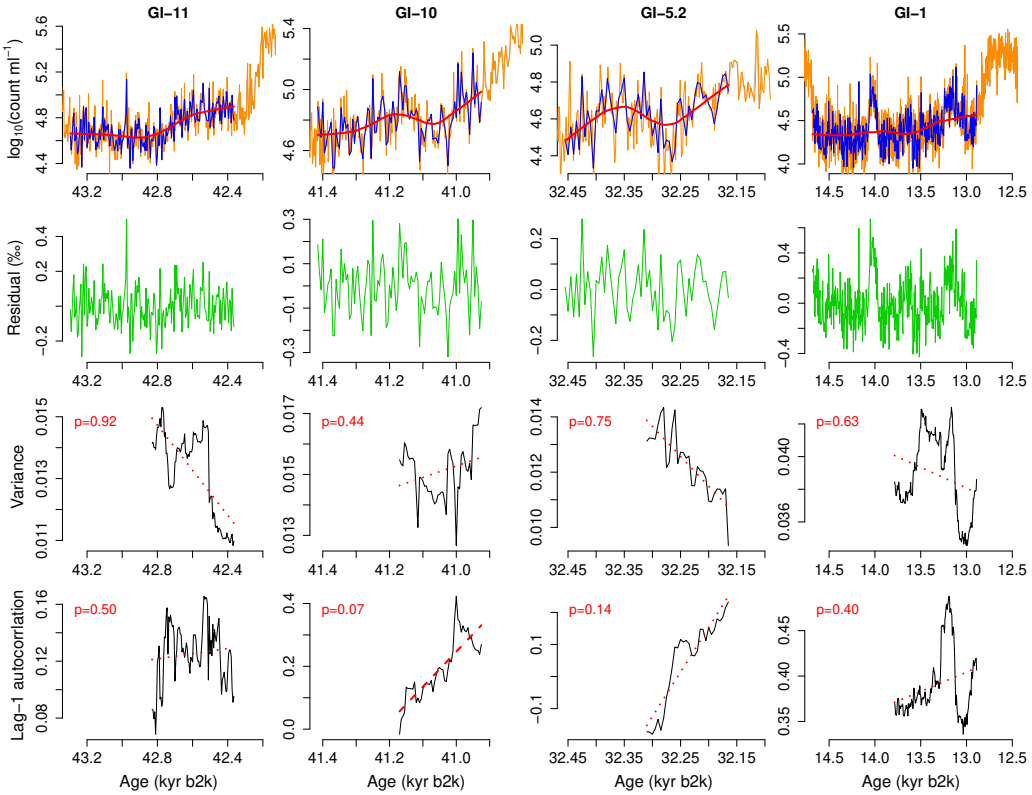

Figure S27. Analysis of CSD-based precursor signals of abrupt DO cooling transitions, for the first half of interglacials of NGRIP 5-cm resolution dust record. (Top row) Interstadial parts longer than 300-yr (blue), which is sampled at every 5-yr from the original data nonuniform in time (orange). The trend calculated with the Locally Weighted Scatterplot Smoothing (LOESS) (red). The smoothing span α that defines the fraction of data points involved in the local linear regression is set to $\alpha = 50\%$ of each interstadial length. (Second row) Residual (green) between the record and the trend. (Third row) Variance in the rolling window (black), size of which is 50% of each interstadial length. The linear trend is shown with the solid red line for $p < 0.05$, with the dashed line for $0.05 < p < 0.1$, and with the dotted line for $p > 0.1$. (Bottom row) Lag-1 autocorrelation.

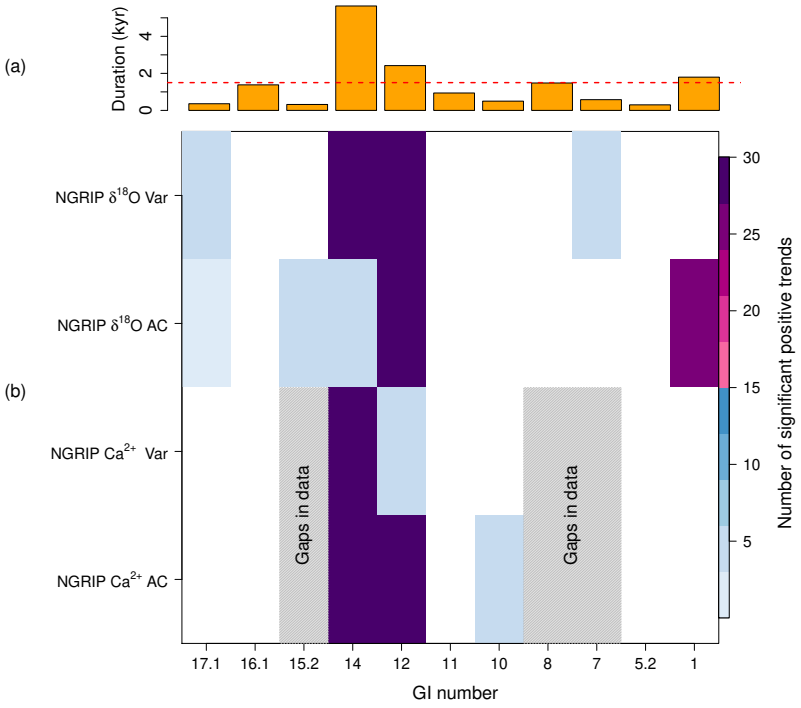

Figure S28. Detection of robust CSD-based precursor signals in interstadials from NGRIP 5-cm resolution δ^{18}O record and dust record. (a) Durations of interstadials longer than 300 yr. The red dashed line shows the level of 1.5 kyr. We find robust precursor signals for interstadials longer than roughly 1.5 kyr. (b) Robustness of finding statistical precursor signals for DO cooling transitions. The color indicates the number of observing a significant trend of CSD indicator ($p < 0.05$) for the 30 sets of the smoothing span and the rolling window size. For the cases of grey-shaded cells, the original data series contain large gaps in time and hence they are excluded from the analysis.

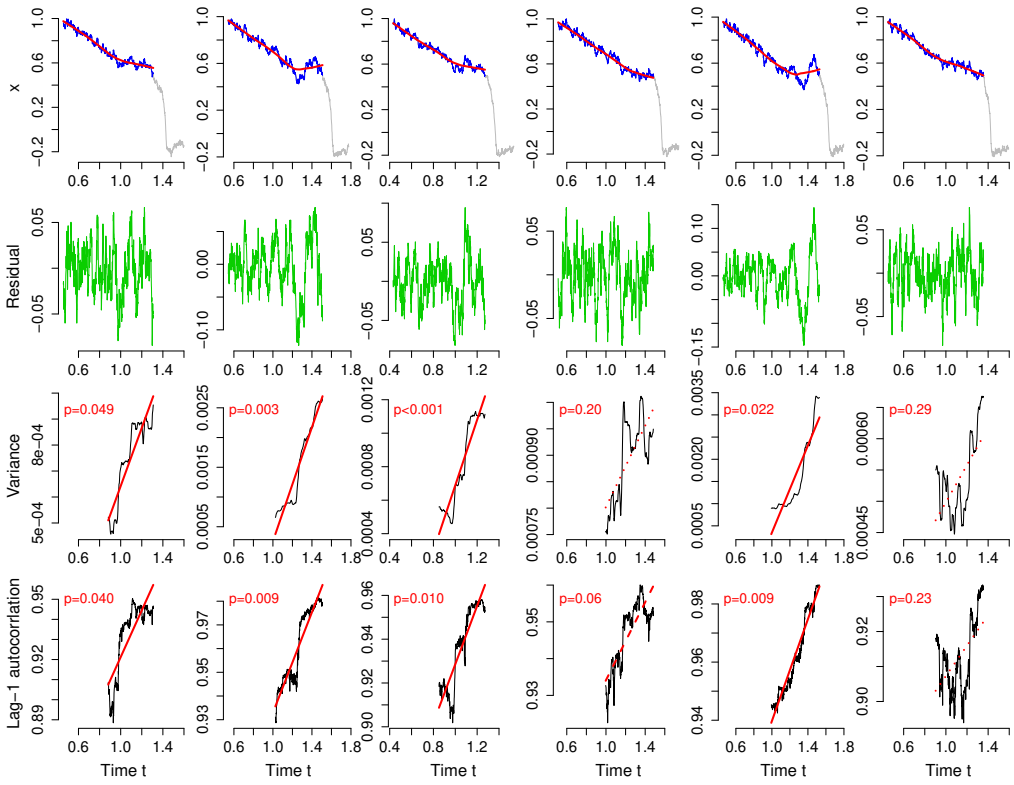

Figure S29. Analysis of CSD-based precursor signals of the downward transition of FitzHugh-Nagumo-type (FHN-type) model. (Top row) The series $x(t)$ before it falls below the critical point at $x = 1/2$ in the last (blue). The latter part (Grey). The trend calculated with the Locally Weighted Scatterplot Smoothing (LOESS) (red). The smoothing span α that defines the fraction of data points involved in the local linear regression is set to $\alpha = 50\%$ of each interstadial length. (Second row) Residual (green) between the record and the trend. (Third row) Variance in the rolling window (black), size of which is 50% of each interstadial length. The linear trend is shown with the solid red line for $p < 0.05$, with the dashed line for $0.05 < p < 0.1$, and with the dotted line for $p > 0.1$. (Bottom row) Lag-1 autocorrelation.

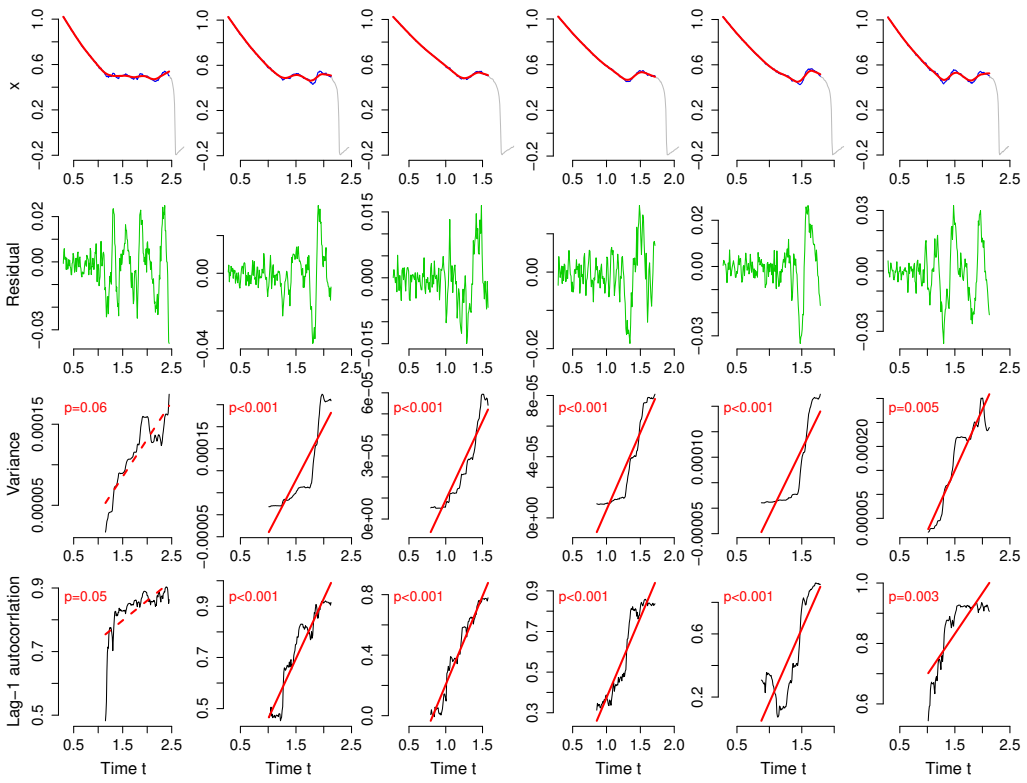

Figure S30. Analysis of CSD-based precursor signals of the Hopf-bifurcation of FitzHugh-Nagumo-type (FHN-type) model. (Top row) The series $x(t)$ before it falls below the critical point at $x = 1/2$ in the last (blue). The latter part (Grey). The trend calculated with the Locally Weighted Scatterplot Smoothing (LOESS) (red). The smoothing span α that defines the fraction of data points involved in the local linear regression is set to $\alpha = 30\%$ of each interstadial length. (Second row) Residual (green) between the record and the trend. (Third row) Variance in the rolling window (black), size of which is 40% of each interstadial length. The linear trend is shown with the solid red line for $p < 0.05$, with the dashed line for $0.05 < p < 0.1$, and with the dotted line for $p > 0.1$. (Bottom row) Lag-1 autocorrelation.

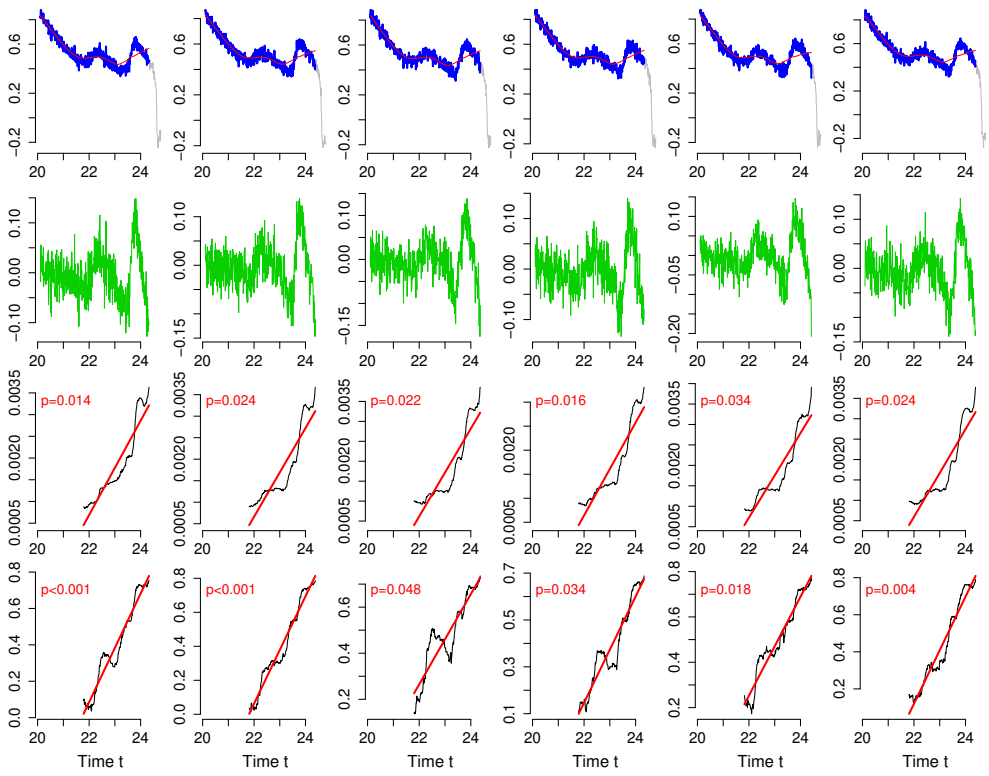

Figure S31. Analysis of CSD-based precursor signals of the downward transition of the mixed-mode oscillation model. (Top row) The series $x(t)$ plus an additive observation noise before it falls below the critical point at $x = 1/2$ in the last (blue). The latter part (Grey). The trend calculated with the Locally Weighted Scatterplot Smoothing (LOESS) (red). The smoothing span α that defines the fraction of data points involved in the local linear regression is set to $\alpha = 40\%$ of each interstadial length. (Second row) Residual (green) between the record and the trend. (Third row) Variance in the rolling window (black), size of which is 40% of each interstadial length. The linear trend is shown with the solid red line for $p < 0.05$, with the dashed line for $0.05 < p < 0.1$, and with the dotted line for $p > 0.1$. (Bottom row) Lag-1 autocorrelation.

References

Rasmussen, S. O., Bigler, M., Blockley, S. P., Blunier, T., Buchardt, S. L., Clausen, H. B., Cvijanovic, I., Dahl-Jensen, D., Johnsen, S. J., Fischer, H., et al. (2014). A stratigraphic framework for abrupt climatic changes during the last glacial period based on three synchronized greenland ice-core records: refining and extending the intimate event stratigraphy. *Quaternary Science Reviews*, 106:14–28.